# Heating/Cooling Stimulus Induces Three-State Molecular Switching of Pseudoenantiomeric Aminomethylenehelicene Oligomers: Reversible Nonequilibrium Thermodynamic Processes

Masanori Shigeno, Yo Kushida, and Masahiko Yamaguchi*

Department of Organic Chemistry, Graduate School of Pharmaceutical Sciences, Tohoku University, Aoba, Sendai 980-8578, Japan

Ⓢ *Supporting Information*

ABSTRACT: A 1:1 mixture of pseudoenantiomeric amino-methylenehelicene (*P*)-tetramer and (*M*)-pentamer formed three states, namely, the heterodouble helices **B** and **C** and the random coil **A**. At high temperatures, **A** is the most stable. At low temperatures, **C** is the most stable, and the structural changes from **A** to the metastable state **B** to the product **C** occur, where **B** and **C** have pseudoenantiomeric helical structures. Heating then converts **C** to **A**. Essentially, all the molecules change their structure from **A** to **B** to **C** to **A**. Various nonequilibrium reversible thermodynamic responses appeared depending on thermal conditions: The metastable states **A** and **B** can be interconverted with thermal hysteresis without forming **C** in a far-from-equilibrium manner; three-state hysteresis occurs; states **A** and **B** can be frozen at low temperatures and defrosted by warming. An energy and population model for the three-state switching is given, involving inversion of thermodynamic stability and thermal hysteresis.

Single thermal stimulus of heating and cooling
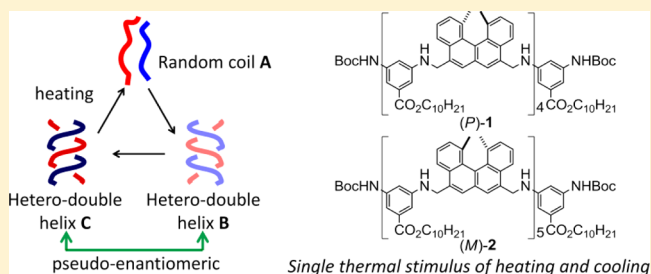
INTRODUCTION

Molecular switching is a reversible function for changing molecular states in response to external stimuli or energy changes, and many examples of switching between two molecular states are known.[1] Multiple-state switching between three or more states using a single molecular substance is attractive for molecular devices and machines, because it can provide more information than two-state systems.[2,3] Such multiple-state switching systems exist in molecular motors of biological cells, and work on the mechanics during the multiple-state molecular transformation using external chemical energy.[1f−h] To understand biological phenomena and to develop related molecular devices and machines, synthetic molecular systems with such switching properties have been examined.[2c−f,h,i,k,3b,c,e,f,h,i]

Three-state switching is the basis of the above multiple-state switching systems, where three states, i.e., **A**, **B**, and **C**, can be taken in response to external stimuli. In addition, along with a reversible change of states from **A** to **B** to **C** to **A**, changes between two states can also occur in the **A** to **B** to **A** mode or **A** to **C** to **A** mode depending on the stimulation conditions.[2a,g,j,3h] Conventional three-state switching entails two or three stimuli with large energies using light, an acid, a base, an oxidant, a reductant, a metal ion, or another chemical reagent in order to induce covalent bond rearrangement (Figure 1a,b). One reason for supplying a large energy is to make each state thermodynamically stable in a reversible three-state system with the **A** to **B** to **C** to **A** reaction.

Heat is a convenient source of energy and usually has a smaller energy under close to ambient conditions than chemical and light energies. Thus, it is interesting to develop a molecular three-state switching system, i.e., **A** to **B** to **C** to **A**, induced by a single thermal stimulus, which saves energy. Although two-state switching using a single thermal stimulus is known,[4] it is not straightforward to consider three-state switching in a closed system, where there is no exchange of chemical substances. For example, in the case that **B** is a kinetic product[5] and **C** is a thermodynamic product, the **A** to **B** to **C** reaction occurs. The relative thermodynamic stability, however, increases in the order **A** < **B** < **C**, and the **C** to **A** reaction is thermodynamically unfavorable.

In this work, we describe a three-state switching system in solution induced by a single cycle of heating and cooling. Essentially all the molecules change their states from **A** to **B** to **C** to **A**, where **A** is the stable form at high temperatures and **C** is the stable form at low temperatures (Figure 1c). One advantage of this system is that various thermal responses appear during the changes of the three states depending on the conditions and history of the thermal stimulus, which are noted as reversible nonequilibrium thermodynamic processes.[6]

RESULTS AND DISCUSSION

Three-State Change A to B to C to A. We have recently synthesized aminomethylenehelicene oligomers and showed their homodouble-helix formation.[7] In this study, the heterodouble-helix formation[8] of a 1:1 mixture of pseudoe-
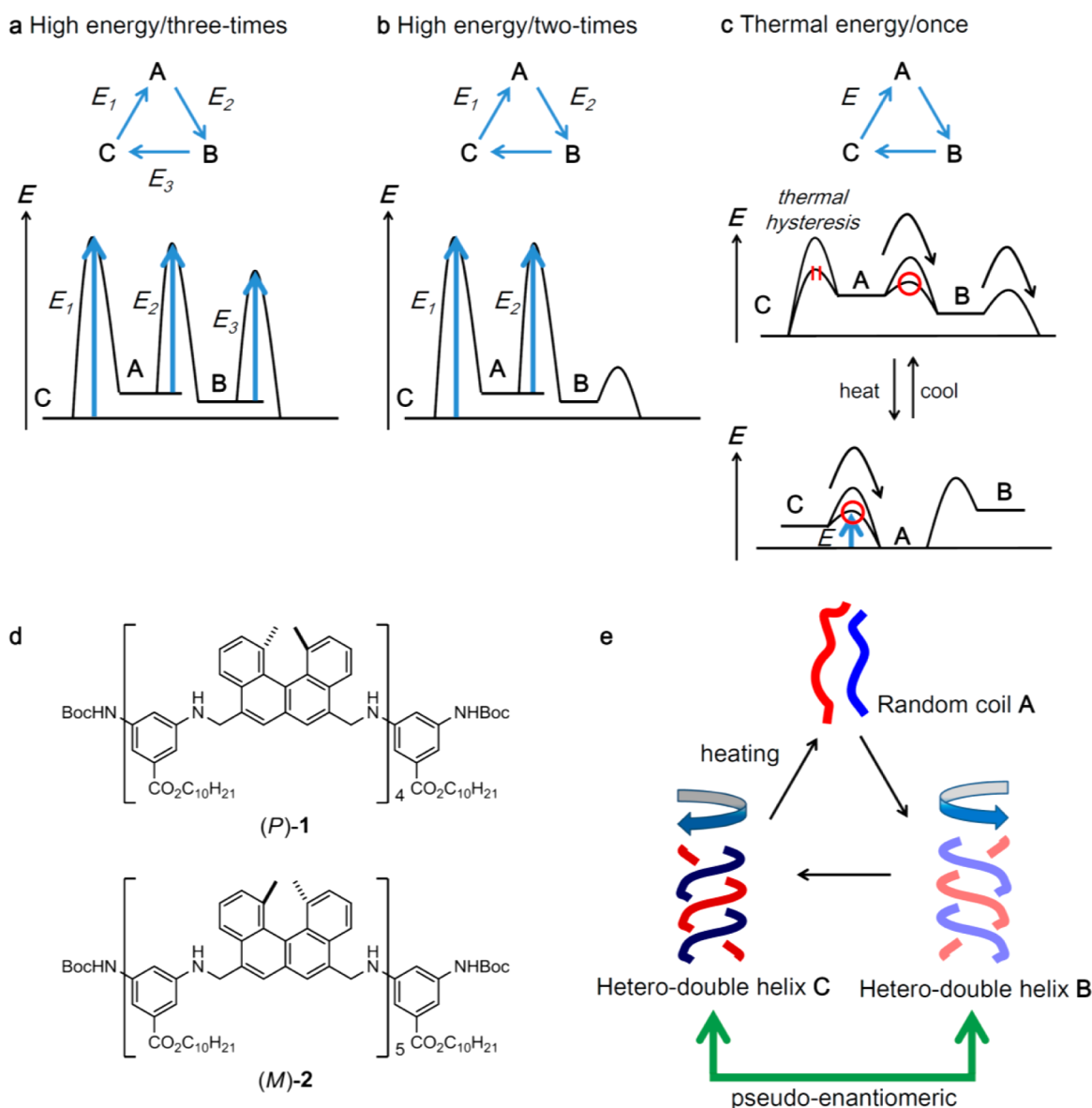
Figure 1. Schematic presentation of models for three-state structural change. (a) High-energy/three-stimulus mode. Three high-energy external stimuli E_1, E_2, and E_3 are provided. (b) High-energy/two-stimulus mode. Two high-energy external stimuli E_1 and E_2 are provided. See also ref 1e, page 98 for the related discussion. (c) Low-energy/single-stimulus mode. (d) The structures of (*P*)-**1** and (*M*)-**2**. (e) Three-state change of **A** to **B** to **C** to **A** using (*P*)-**1**/(*M*)-**2** system.

nantiomeric helicene tetramer (*P*)-**1** and pentamer (*M*)-**2** containing an aminomethylene linker was examined (Figure 1d), which exhibited a three-state change in solution between the random coil **A**, the heterodouble helix **B**, and the heterodouble helix **C** (Figure 1e). **A** is in a high-energy state at low temperatures, and **B** and **C**, possessing a pseudoenantiomeric nature, are in metastable[5] and stable states, respectively (Figure 1c). Then, a structural change occurs by **A** to **B** to **C**. **C** thus formed is dissociated to **A** by heating, which contains an inversion of the relative thermodynamic stability of **A** and **C**.[9] Essentially, all the molecules then undergo the overall three-state change from **A** to **B** to **C** to **A** with a single cooling/heating operation, which contains thermal hysteresis.[10]

Three states were obtained for a 1:1 mixture of pseudoenantiomeric (*P*)-**1** and (*M*)-**2** (total concentration 5.0 × 10⁻⁴ M) in fluorobenzene during heating and cooling. At 70 °C, both compounds are **A**, which is determined by the

coincidence of the experimental CD and UV−vis spectra with the calculated spectra obtained from the random coil of (*P*)-**1** and (*M*)-**2** (blue and red lines in Figure 2a,b, and Supporting Information, (SI) S1). VPO analysis (60 °C, 5.0 × 10⁻⁴ M) provided the average molecular weight of the two compounds [(2.8 ± 0.1) × 10³ (calcd. 3071)], and DLS (70 °C, 1.0 × 10⁻³ M) gave an average diameter of 1 nm for the substances in solution (SI Figure S2). Thus, essentially all the molecules are **A** without other aggregates, and the equilibrium-shifted state was noted to be the S-random coil **A** in this study.

When the solution was cooled to 25 °C and allowed to settle for 20 min, the CD spectra reached a state with strong positive and negative Cotton effects at 300 and 315 nm, respectively (green line in Figures 2a and SI S4a) with two isosbestic points at 308 and 355 nm. The above results indicated the formation of an ordered structure, that is, the heterodouble helix **B** from the random coil **A**. UV−vis analysis showed a long-wavelength
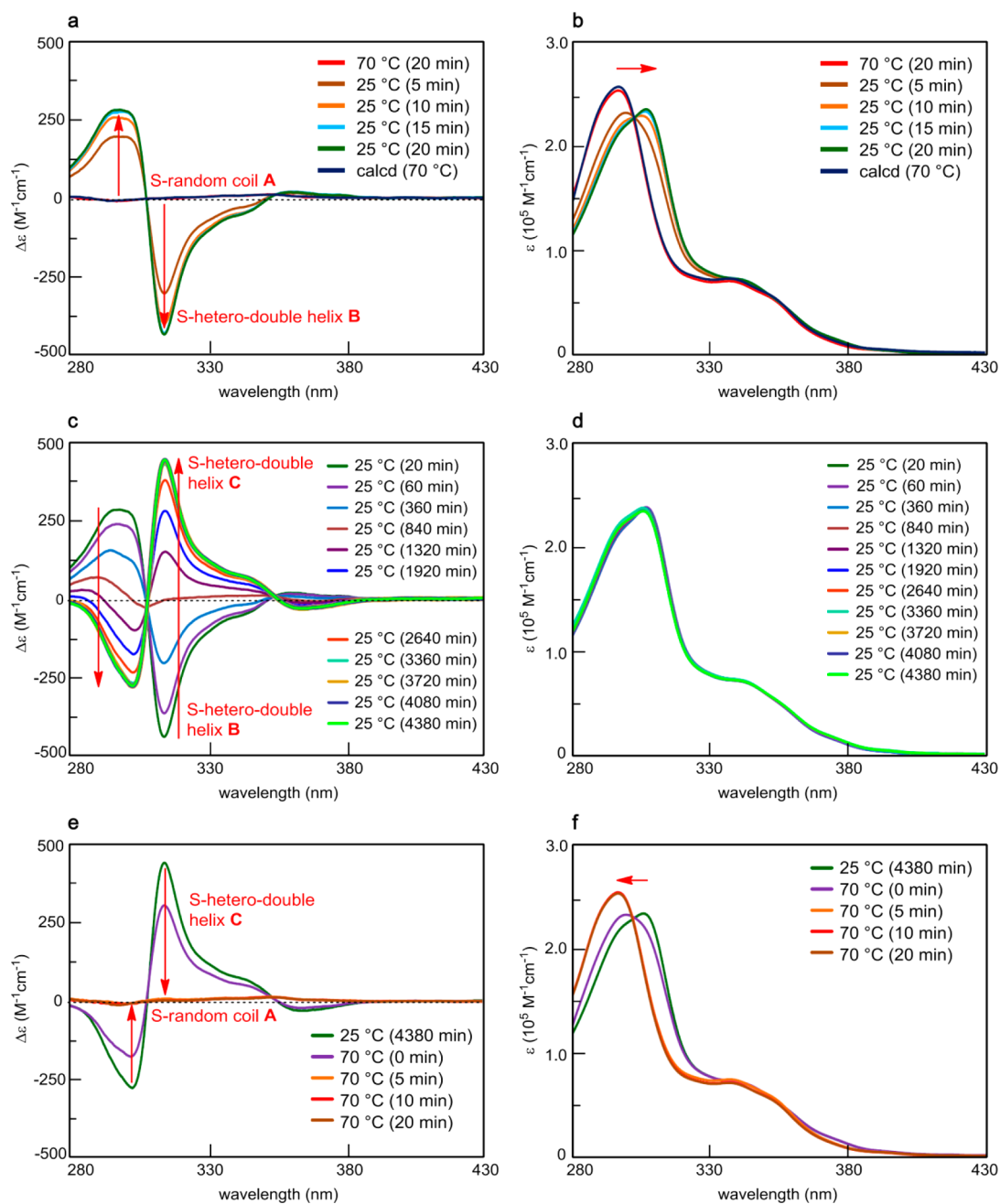
Figure 2. CD spectra (a, c, e) and UV−vis spectra (b, d, f) (total concentration, 5.0×10^{-4} M; fluorobenzene) of (P)-**1**/(M)-**2** (1:1) mixture in the **A** to **B** to **C** to **A** process. (a, b) The solution was heated at 70 °C (20 min) and cooled to 25 °C (20 min). The calculated spectrum was obtained by adding the spectra of (P)-**1** and (M)-**2** (fluorobenzene, 5.0×10^{-4} M; 70 °C) and dividing the sum by two. (c, d) The solution (a, b) was allowed to settle at 25 °C for the time indicated, and CD and UV−vis spectra were obtained. (e, f) The solution (c, d) was heated to 70 °C for 20 min.

shift of the absorption maximum from 298 to 307 nm (Figures 2b and SI S4b). DLS (25 °C, 1.0×10^{-3} M) showed an average diameter of 6 nm for the particles, which was much larger than that of the random coil **A** (SI Figure S5). VPO (40 °C, 1.5×10^{-3} M, within 60 min) provided an apparent molecular weight of $(6.2 \pm 0.2) \times 10^3$ (calcd. 6141), which indicated the heteroaggregate formation of (P)-**1** and (M)-**2**. The Job plots experiment (50 °C, total concentration 1.0×10^{-3} M) showed the formation of a 1:1 complex (SI Figure S6). The CD spectra were obtained at different temperatures and concentrations and exhibited a convergence to a single spectrum at lower temperatures and higher concentrations, i.e., 25 °C (5.0×10^{-4} M), 5/25 °C (1.0×10^{-3} M), and 40 °C (1.5×10^{-3} M)

(SI Figure S4). The spectrum was then assigned to the S-heterodouble helix **B**, which had no other aggregates. As previously noted for pseudoenantiomeric ethynylhelicene oligomers,[8] pseudoenantiomeric aminomethylenehelicene oligomers with another two-atom linker form strong hetero-double helices.

A slow inversion of the CD spectra occurred by allowing the solution (5.0×10^{-4} M) of the S-heterodouble helix **B** to stand at 25 °C for 3360 min, which was accompanied by two isosbestic points at 308 and 356 nm (Figure 2c). The S-heterodouble helix **C** was thermodynamically stable at 25 °C and showed no change after reaching the steady state (SI Figures S26 and S27). The UV−vis spectra showed no change
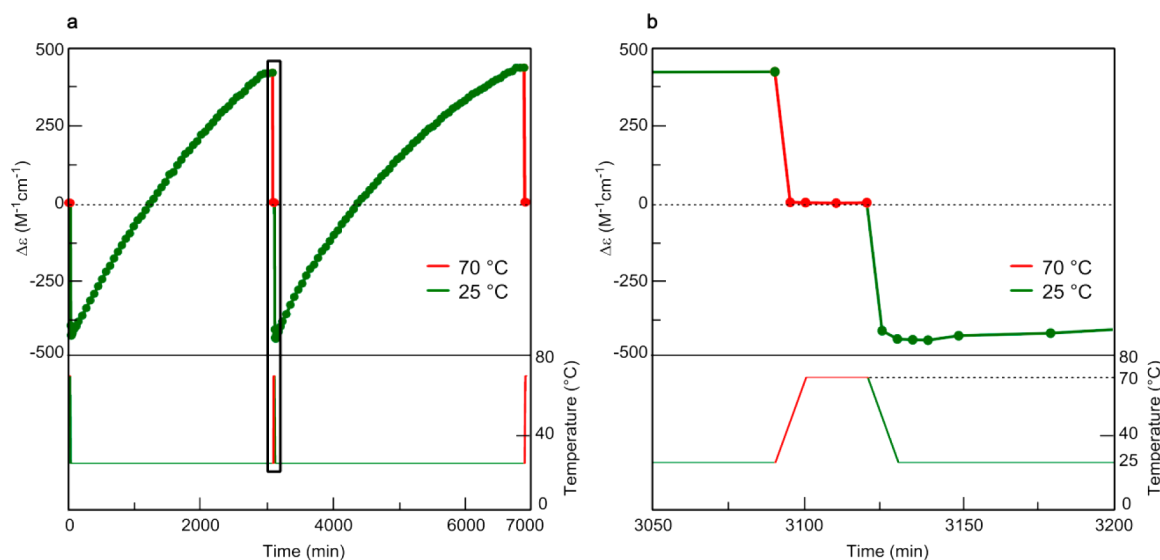
Figure 3. $\Delta\varepsilon$ (315 nm)/time profile (a) of (P)-**1**/(M)-**2** (1:1, total concentration, 1.0×10^{-3} M; fluorobenzene) for repeated cycles of heating at 70 °C (red line), and cooling at 25 °C (green line). Part (b) shows the expansion of the profile between 3050 and 3200 min.

during the process (Figure 2d). The VPO (40 °C, total concentration 1.5×10^{-3} M) of the resulting solution showed heteroaggregate formation $[(6.0 \pm 0.3) \times 10^3 \text{ (calcd 6141)}]$, and DLS (25 °C, 1.0×10^{-3} M) provided an average diameter of 6 nm for the substances (SI Figure S9). The Job plots experiment (fluorobenzene, 1.0×10^{-3} M) showed a 1:1 complex formation (SI Figure S10). Thus, another hetero-double helix, **C**, was formed after 40 h at 25 °C, and the heterodouble helices **B** and **C** turned out to be pseudoenantiomeric. The helicenes in (P)-**1** and (M)-**2** do not racemize below 200 °C.[11] It is then due to the pseudoenantiomeric nature of the three-dimensional structures of double helices that the CD spectra of the heterodouble helix **B** and the heterodouble helix **C** appear in mirror-image.

Kinetic study indicated the monomolecular nature of the reaction with a rate constant $k = (8.7 \pm 0.1) \times 10^{-4}$ min^{-1} (fluorobenzene, 25 °C, 5.0×10^{-4} M) (SI Figures S11 and S12). The isosbestic points in the CD spectra (Figure 2C) and the apparent first-order kinetics are consistent with the structural change between two states of heterodouble helix **C** and heterodouble helix **B**. With regard to molecular mechanism in the **B** to **C** reaction, dissociation of **B** to **A** may be contained.

The convergence of CD spectra was observed for the heterodouble helix **C** by analysis at different concentrations and temperatures (SI Figure S8), and the spectrum was assigned to the S-heterodouble helix **C** without other aggregates. Thus, essentially all the molecules changed their structure from **A** to **B** to **C**. It may also be worth noting that the inversion of the helical sense contained in the **B** to **C** process occurs spontaneously without external stimuli. It is different from most known helical-sense inversion of oligomers and polymers,[12,13] induced generally by external stimuli of temperature, solvent, light, and additives.

C was converted to **A** by heating the fluorobenzene solution (5.0×10^{-4} M) to 70 °C, as indicated by the decrease in CD intensity with two isosbestic points at 309 and 355 nm (Figure 2e). UV−vis spectra showed a shift in absorption maxima to a shorter wavelength (Figure 2f). Kinetic study on this process also indicated the monomolecular nature of the reaction with a rate constant $k = (1.59 \pm 0.01) \times 10^{-2}$ s^{-1} (fluorobenzene, 60

°C, 5.0×10^{-4} M) (SI Figures S13 and S14). The results indicated that essentially all the molecules were converted from **C** to **A** during the heating process. The overall process provided a three-state change from **A** to **B** to **C** to **A**, induced by a single cooling/heating operation (Figure 1e). The single stimulus nature of the process is clearly shown by the repeated switching experiment, in which a mixture of (P)-**1**/(M)-**2** in fluorobenzene (total 1.0×10^{-3} M) was heated at 70 °C (30 min), cooled to 25 °C (51 h), heated at 70 °C (30 min), cooled to 25 °C (63 h), and heated at 70 °C (30 min) (Figure 3).

Constant-Rate Temperature Change Experiments. To compare the nonequilibrium process of the three-state change, equilibrium states were determined by heating the solution (5 °C, 5.0×10^{-4} M) of the S-heterodouble helix **C** to 25, 40, 45, 50, 55, 60, and 70 °C in this order, and obtaining its CD spectrum in the steady state at each temperature (SI Figure S15). The results were rearranged to a $\Delta\varepsilon$ (315 nm)/temperature profile, which showed the formation of **A** above 60 °C under equilibrium, and **C** below 25 °C (purple lines in Figure 4).[14]

Constant-rate temperature change experiments were conducted by analyzing the $\Delta\varepsilon$ at 315 nm in the mixture of (P)-**1** and (M)-**2** (total concentration, 5.0×10^{-4} M) in fluorobenzene, which exhibited a different responses depending on thermal conditions. The $\Delta\varepsilon$ values of 3, −430, and 440 M^{-1}cm^{-1} were used for those of the S-random coil **A**, the S-heterodouble helix **B**, and the S-heterodouble helix **C**, respectively (SI Figures S1, S4, and S8). The change from **C** to **A** to **B** was achieved by increasing the temperature from 5 to 70 °C and then decreasing it from 70 to 5 °C at a rate of 2 K/min (Figure 4a). During heating from 30 to 60 °C, $\Delta\varepsilon$ decreased from 440 to 3 M^{-1}cm^{-1}, and remained constant above 60 °C. The heating curve was similar to the equilibrium curve noted above. Notably, cooling from 70 to 5 °C followed quite a different process, and $\Delta\varepsilon$ decreased from 3 to −430 M^{-1}cm^{-1}, yielding **B**. The **C** to **A** to **B** reaction induced by heating and cooling exhibits thermal hysteresis.

Another constant-rate experiment was conducted starting from the S-random coil **A** at 70 °C. The solution was cooled from 70 to 5 °C and then heated to 70 °C at a rate of 1.5 or 2
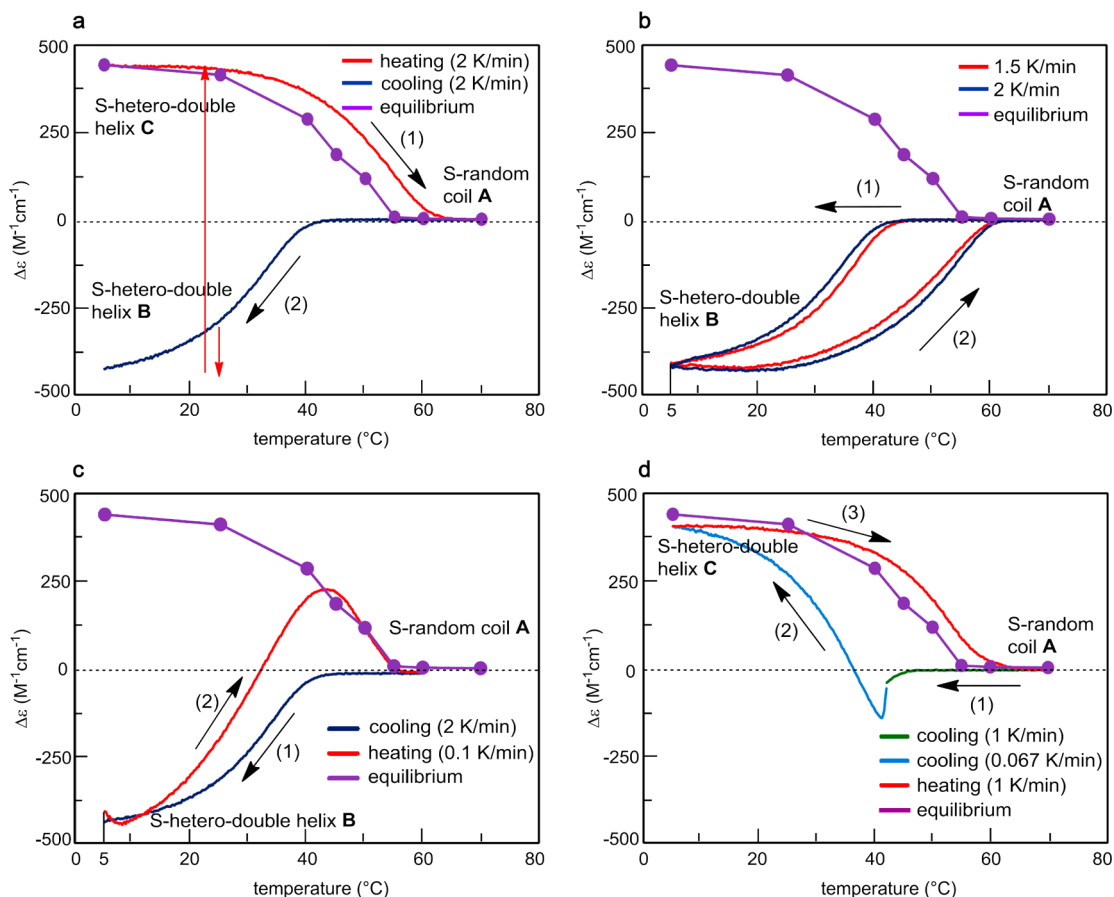
Figure 4. $\Delta\varepsilon$ (315 nm)/temperature profiles of (P)-**1** and (M)-**2** (1:1) in fluorobenzene (5.0×10^{-4} M) at heating/cooling rates of 1.5 and 2 K/min, and three-state thermal hysteresis shown by $\Delta\varepsilon$ (315 nm)/temperature profiles. (a) $\Delta\varepsilon$ (315 nm)/temperature profiles of (P)-**1** and (M)-**2** (1:1) in fluorobenzene (5.0×10^{-4} M) at heating/cooling rate of 2 K/min. Temperature was increased from 5 to 70 °C and then decreased from 70 to 5 °C. The arrow shows the experiment in Figures 2a and 2c. $\Delta\varepsilon$ values in equilibrium were obtained (SI Figure S15a), and purple lines are drawn between their points. See SI Figure S20 for UV−vis analysis. (b) $\Delta\varepsilon$ (315 nm)/temperature profiles of (P)-**1** and (M)-**2** (1:1) in fluorobenzene (5.0×10^{-4} M) at heating/cooling rates of 1.5 and 2 K/min. Temperature was decreased from 70 to 5 °C and then increased from 5 to 70 °C. The equilibrium curve is also shown. See SI Figure S22 for UV−vis analysis. (c) Three-state thermal hysteresis shown by $\Delta\varepsilon$ (315 nm)/temperature profiles of (P)-**1**/(M)-**2** (1:1) in fluorobenzene (5.0×10^{-4} M) at a cooling rate of 2 K/min and heating rate of 0.1 K/min. Temperature was decreased from 60 to 5 °C (blue line) and then increased from 5 to 60 °C (red line). See SI Figure S23 for UV−vis analysis. (d) Another three-state thermal hysteresis. (P)-**1** and (M)-**2** (1:1) in fluorobenzene (5.0×10^{-4} M) was cooled from 70 to 42 °C at a rate of 1 K/min, and then to 5 °C at a rate of 0.067 K/min, and heated from 5 to 70 °C at a rate of 1 K/min. See SI Figure S24 for UV−vis analysis.

K/min, where $\Delta\varepsilon$ changed between −430 and 3 $M^{-1}cm^{-1}$ (Figure 4b). Thermal hysteresis was observed in the change between **A** and **B**. Note that, starting from **A**, the system spontaneously departed from equilibrium upon cooling and interconverted with **B**. The process did not show any sign of the formation of **C**, despite **C** being thermodynamically most stable at low temperatures, which is a far-from equilibrium thermodynamic phenomenon.[16]

No formation of **C** was observed under the above conditions because of the relatively high heating rate. When heating was conducted at a low rate of 0.1 K/min, **C** formation was observed during heating, as indicated by the inflated upward curve, showing three-state hysteresis between **A**, **B**, and **C** (Figure 4c).

Another three-state hysteresis curve close to equilibrium was obtained under a different temperature change. The fluorobenzene solution (5.0×10^{-4} M) of the S-random coil **A** at 70 °C was cooled to 42 °C at a rate of 1 K/min and then to 5 °C at a rate of 0.067 K/min, and heated to 70 °C at a rate of 1 K/min (Figure 4d). The change from **A** to **B** to **C** was observed,

as indicated by a downward spike in $\Delta\varepsilon$ of −138 $M^{-1}cm^{-1}$ at 40.8 °C followed by an increase in $\Delta\varepsilon$ to 410 $M^{-1}cm^{-1}$.

These are from molecular thermal hysteresis,[10] in which the molecular state spontaneously departs from equilibrium upon cooling.[6] Although thermal hysteresis containing metastable states is known for bulk materials[15] such as condensed phases of polymer aggregates, gels, and crystals, molecular thermal hysteresis in solution is rare, as noted in our previous study.[10]

Frozen/Defrost Experiments. It was found that the metastable S-heterodouble helix **B** and the S-random coil **A** could be frozen at low temperatures by appropriate thermal treatments (Figure 5a,d). This indicates that three S-states of the molecules in solution can be stored. **B** was frozen by decreasing the temperature from 70 to −10 °C at a rate of 2 K/min, and the state was stable for at least 8 h (SI Figures S28 and S29). When the frozen solution at −10 °C was warmed to 25 °C (defrost), a slow conversion to **C** occurred (Figures 5b,c and SI S30, S31, and S32). In another experiment, **A** was frozen by the snap cooling of the solution from 70 to −35 °C, and then to −30 °C, and the CD spectra did not change for 15 min at −30 °C (Figures 5e and SI S33). **A** at −30 °C was defrosted
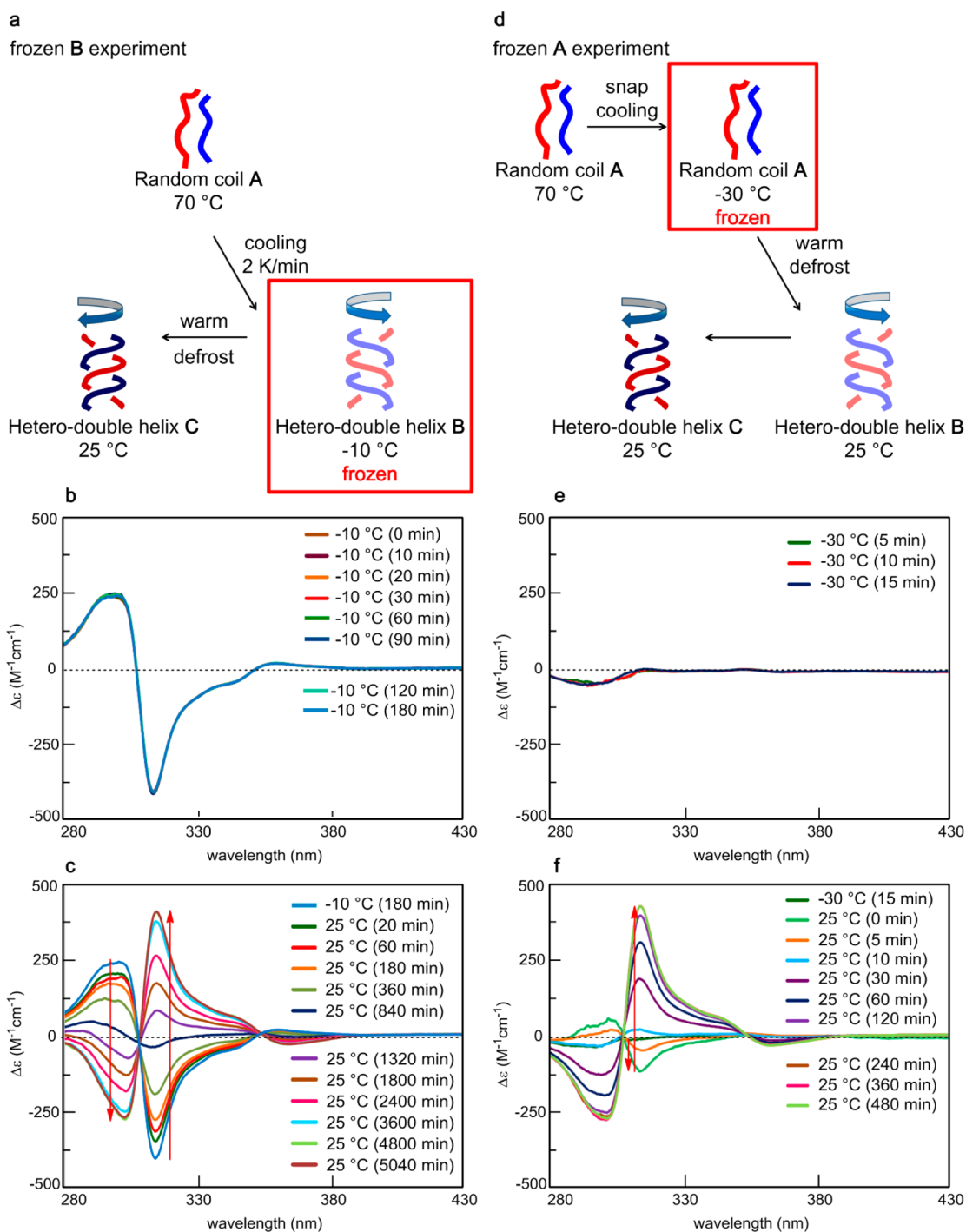
Figure 5. Frozen/defrost experiments of **A** and **B**. Schemes for the frozen/defrost experiments of **A** (a) and **B** (d). CD spectra of (b) frozen and (c) defrosted S-heterodouble helices **B** of (P)-**1**/(M)-**2** (1:1) (total concentration, 5.0×10^{-4} M; fluorobenzene); CD spectra of (e) frozen and (f) defrosted S-random coils **A** of (P)-**1**/(M)-**2** (1:1) (total concentration, 5.0×10^{-4} M; fluorobenzene). (b, c) The solution was cooled from 70 to -10 °C at a rate of 2 K/min, allowed to settle at -10 °C for 3 h, warmed to 25 °C, and again allowed to settle at 25 °C for 84 h. (e, f) The solution was cooled from 70 to -35 °C, allowed to settle at -35 °C for 5 min, warmed to -30 °C, allowed to settle at -30 °C for 15 min, warmed to 25 °C, and finally allowed to settle at 25 °C for 8 h. Also see SI Figures S28−S35.

by warming to 25 °C, which induced a structural change to **B** and then to **C** (Figures 5f and SI S34 and S35). Unlike conventional dimeric aggregate formation, which occurs at lower temperatures, the aggregates **B** and **C** are formed by warming the frozen **A**.

To summarize the experiments, the (P)-**1**/(M)-**2** system provides a novel experiment system of nonequilibrium thermodynamics at the molecular level. Under controlled conditions, the **A** to **B** to **C** to **A** changes between the S-states took place. During a relatively fast temperature change, **A** and **B** interconverted with each other without forming **C**, being at the global energy minimum. Three-state hysteresis was observed under slow-temperature-change conditions. The frozen states **A** and **B**, having local energy minima, were obtained at low temperatures, which could be defrosted by warming to give **C**. Depending on the cooling/heating rate and thermal history, the
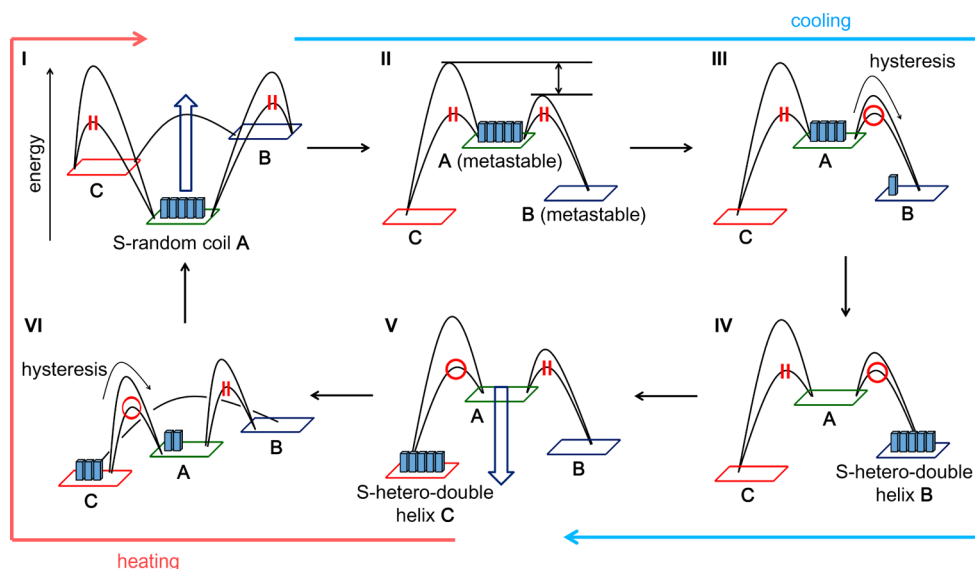
Figure 6. Model of three-state switching **A** to **B** to **C** to **A**. The relative populations of molecules in the **A**, **B**, and **C** structures are shown by blue cubes. The relative thermodynamic stability of three states is **A** > **C** > **B** at high temperature (state I) and **C** > **B** > **A** at low temperature (states II, III, IV, and V). The model contains two transition states of low-barrier path and high-barrier path in the **A** to **B** reaction (states II and III) and the **C** to **A** reaction (states V, VI, and I). The low-barrier paths open when the products **B** or **C** are present in the solution, and otherwise only the high-barrier path is open (self-catalysis). See ref 10 for details of the switching in the transition states in the thermal hysteresis. The model explains the energy/polpulation of the three-state switching **A** to **B** to **C** to **A**, and not the molecular mechanism.

(*P*)-**1**/(*M*)-**2** system exhibits various thermal responses, and the results provide experimental insights into reversible nonequilibrium thermodynamic systems, which are common and very complex in the real world but not well-known at the molecular level.

Model of Three-State Switching. On the basis of the results of the above experiments and our recent discussions of inversion of the relative thermodynamic stability[9] and two-state thermal hysteresis,[10] the three-state switching **A** to **B** to **C** to **A** was explained by a model on the basis of four assumptions: (1) The relative thermodynamic stability remains **C** > **B**. (2) The relative thermodynamic stability of **A** changes between **A** > **C** > **B** at high temperatures and **C** > **B** > **A** at low temperatures.[9] (3) The coordinates of reaction between **C** and **A** contain high- and low-barrier paths due to thermal hysteresis.[10] (4) The coordinates of reaction between **A** and **B** also contain high- and low-barrier paths due to thermal hysteresis.[10]

At high temperatures, **A** is thermodynamically the most stable, and all the molecules remain as the S-random coil **A** (Figure 6, state I). As the temperature decreases, the thermodynamic stability changes to **C** > **B** > **A**, but the molecules remain as **A** because of thermal hysteresis (state II). It is due to the presence of a high-energy barrier for forming **C** from **A** and for forming **B** from **A**, where the low-barrier paths are closed. Since the barrier is lower for the formation of **B** than of **C**, molecules are slowly converted to **B** (state III). Then, a low-barrier path opens after an induction period, which converts all the molecules to **B** likely via self-catalysis, i.e., **B** catalyzes the formation of **B** from **A**[10] (state IV). A slow change from the metastable S-heterodouble helix **B** to the S-heterodouble helix **C** follows (state V). Heating converts all the molecules of **C** to **A** by changing thermodynamic stability to **A** > **C** > **B** (states VI and I). Nonequilibrium thermodynamics implies the inconsistency of the relative energy levels and the Boltzmann distribution of molecular

populations (see, state II), and vice versa, equilibrium thermodynamics.

CONCLUSIONS

In summary, a 1:1 mixture of a pseudoenantiomeric amino-methylenehelicene (*P*)-tetramer and an (*M*)-pentamer formed three S-states, namely, the heterodouble helices **B** and **C** and the random coil **A**, in fluorobenzene, which thermally interconverted into each other. At high temperatures, **A** is most stable, and both the tetramer and the pentamer remain in the random coil state. At low temperatures, **C** is the most stable, and the structural change from **A** to **C** takes place via the metastable intermediate **B**. The heterodouble helices **B** and **C** have pseudoenantiomeric structures with regard to their helical nature. The overall transformation provides a three-state switching, **A** to **B** to **C** to **A** in a closed system. Various thermal responses appear, depending on the conditions and history (time dependent) of thermal stimuli, which are notable in the experiments on nonequilibrium thermodynamic processes at the molecular level. An energy and population model for explaining the phenomenon is given, which contains two metastable states and thermal hysteresis.

Compared to conventional three-state molecular switching systems, the present system has a property of employing a single thermal stimulation and exhibiting diversity of responses. A disadvantage may be that one of the states is a random-coil, lacking structure. Development of a system containing a three ordered structure system is an interesting subject for future research.

ASSOCIATED CONTENT

Ⓢ Supporting Information

Full experimental details, including general methods, synthesis, analysis, and additional references. This material is available free of charge via the Internet at http://pubs.acs.org.

■ REFERENCES

(1) (a) Feringa, B. L., Ed. *Molecular Switches*; Wiley-VCH: Weinheim, 2001. (b) Schliwa, M., Ed. *Molecular Motors*; Wiley-VCH: Weinheim, 2003. (c) Kinbara, K.; Aida, T. *Chem. Rev.* **2005**, *105*, 1377. (d) Balzani, V.; Credi, A.; Raymo, F. M.; Stoddart, J. F. *Angew. Chem., Int. Ed.* **2000**, *39*, 3348. (e) Kay, E. R.; Leigh, D. A.; Zerbetto, F. *Angew. Chem., Int. Ed.* **2007**, *46*, 72. (f) Vale, R. D.; Milligan, R. A. *Science* **2000**, *288*, 88. (g) Mahadevan, L.; Matsudaira, P. *Science* **2000**, *288*, 95. (h) van den Heuvel, M. G. L.; Dekker, C. *Science* **2007**, *317*, 333. (i) Coronado, E.; Gaviña, P.; Tatay, S. *Chem. Soc. Rev.* **2009**, *38*, 1674. (j) Coskun, A.; Spruell, J. M.; Barin, G.; Dichtel, W. R.; Flood, A. H.; Botros, Y. Y.; Stoddart, J. F. *Chem. Soc. Rev.* **2012**, *41*, 4827.

(2) For examples of molecular switching employing three times or more stimuli, see: (a) Lawson, M.; Eisler, S. *Org. Biomol. Chem.* **2012**, *10*, 8770. (b) Haberhauer, G. *Angew. Chem., Int. Ed.* **2011**, *50*, 6415. (c) Markey, M. D.; Kelly, T. R. *Tetrahedron* **2008**, *64*, 8381. (d) Kelly, T. R.; Cai, X.; Damkaci, F.; Panicker, S. B.; Tu, B.; Bushell, S. M.; Cornella, I.; Piggott, M. J.; Salives, R.; Cavero, M.; Zhao, Y.; Jasmin, S. *J. Am. Chem. Soc.* **2007**, *129*, 376. (e) Marlin, D. S.; Cabrera, D. G.; Leigh, D. A.; Slawin, A. M. *Angew. Chem., Int. Ed.* **2006**, *45*, 77. (f) Fletcher, S. P.; Dumur, F.; Pollard, M. M.; Feringa, B. L. *Science* **2005**, *310*, 80. (g) Browne, W. R.; de Jong, J. J. D.; Kudernac, T.; Walko, M.; Lucas, L. N.; Uchida, K.; van Esch, J. H.; Feringa, B. L. *Chem.—Eur. J.* **2005**, *11*, 6430. (h) Lin, Y.; Dahl, B. J.; Branchaud, B. P. *Tetrahedron Lett.* **2005**, *46*, 8359. (i) Leigh, D. A.; Wong, J. K. Y.; Dehez, F.; Zerbetto, F. *Nature* **2003**, *424*, 174. (j) Raymo, F. M.; Giordani, S.; White, A. J. P.; Williams. *J. Org. Chem.* **2003**, *68*, 4158. (k) Kelly, T. R.; Silva, R. A.; Silva, H. D.; Jasmin, S.; Zhao, Y. *J. Am. Chem. Soc.* **2000**, *122*, 6935. (l) Pina, F.; Roque, A.; Melo, M. J.; Maestri, M.; Belladelli, L.; Balzani, V. *Chem.—Eur. J.* **1998**, *4*, 1184.

(3) For examples of molecular switching employing twice stimuli, see: (a) Nishikawa, M.; Kume, S.; Nishihara, H. *Phys. Chem. Chem. Phys.* **2013**, *15*, 10549. (b) Ruangsupapichat, N.; Pollard, M. M.; Harutyunyan, S. R.; Feringa, B. L. *Nat. Chem.* **2011**, *3*, 53. (c) Wang, J.; Feringa, B. L. *Science* **2011**, *331*, 1429. (d) Stępień, M.; Szyszko, B.; L.-Grażyński, L. *J. Am. Chem. Soc.* **2010**, *132*, 3140. (e) Pijper, D.; Feringa, B. L. *Angew. Chem., Int. Ed.* **2007**, *46*, 3693. (f) Browne, W. R.; Pollard, M. M.; de Lange, B.; Meetsma, A.; Feringa, B. L. *J. Am. Chem. Soc.* **2006**, *128*, 12412. (g) Kume, S.; Murata, M.; Ozeki, T.; Nishihara, H. *J. Am. Chem. Soc.* **2005**, *127*, 490. (h) Bottari, G.; Dehez, F.; Leigh, D. A.; Nash, P. J.; Pérez, E. M.; Wong, J. K. Y.; Zerbetto, F. *Angew. Chem., Int. Ed.* **2003**, *42*, 5886. (i) Cardenas, D. J.; Livoreil, A.; Sauvage, J.-P. *J. Am. Chem. Soc.* **1996**, *118*, 11980. See also: (j) Perera, U. G. E.; Ample, F.; Kersell, H.; Zhang, Y.; Vives, G.; Echeverria, J.; Grisolia, M.; Rapenne, G.; Joachim, C.; Hla, S.-W. *Nat. Nanotech.* **2012**, *8*, 46.

(4) For recent examples, see: (a) Zalibera, M.; Jalilov, A. S.; Stoll, S.; Guzei, I. A.; Gescheidt, G.; Nelsen, S. F. *J. Phys. Chem. A* **2013**, *117*, 1439. (b) Yamada, H.; Wu, Z.-Q.; Furusho, Y.; Yashima, E. *J. Am. Chem. Soc.* **2012**, *134*, 9506. (c) Eggenspiller, A.; Takai, A.; EI-Khouly, M. E.; Ohkubo, K.; Gros, C. P.; Bernhard, C.; Goze, C.; Denat, F.; Barbe, J.-M.; Fukuzumi, S. *J. Phys. Chem. A* **2012**, *116*, 3889. (d) Yoon, M.-C.; Kim, P.; Yoo, H.; Shimizu, S.; Koide, T.; Tokuji, S.; Saito, S.; Osuka, A.; Kim, D. *J. Phys. Chem. B* **2011**, *115*, 14928. (e) Sugiura, H.; Amemiya, R.; Yamaguchi, M. *Chem.—Asian J.* **2008**, *3*, 244. (f) Stępień, M.; Latos-Grażyński, L.; Sprutta, N.; Chwalisz, P.; Szterenberg, L. *Angew. Chem., Int. Ed.* **2007**, *46*, 7869. (g) Berl, V.; Huc, I.; Khoury, R. G.; Krische, M. J.; Lehn, J.-M. *Nature* **2000**, *407*, 720.

(5) (a) Fahrenbach, A. C.; Zhu, Z.; Cao, D.; Liu, W.-G.; Li, H.; Dey, S. K.; Basu, S.; Trabolsi, A.; Botros, Y. Y.; Goddard, W. A., III; Stoddart, J. F. *J. Am. Chem. Soc.* **2012**, *134*, 16275. (b) Gan, Q.; Ferrand, Y.; Chandramouli, N.; Kauffmann, B.; Aube, C.; Dubreuil, D.; Huc, I. *J. Am. Chem. Soc.* **2012**, *134*, 15656. (c) Cangelosi, V. M.; Carter, T. G.; Zakharov, L. N.; Johnson, D. W. *Chem. Commun.* **2009**, 5606. (d) Kajitani, T.; Okoshi, K.; Sakurai, S.; Kumaki, J.; Yashima, E. *J. Am. Chem. Soc.* **2006**, *128*, 708. (e) Levin, M. D.; Stang, P. J. *J. Am. Chem. Soc.* **2000**, *122*, 7428. (f) Hasenknopf, B.; Lehn, J.-M.; Boumediene, N.; Leize, E.; Van Dorsselaer, A. *Angew. Chem., Int. Ed.* **1998**, *37*, 3265. See also: (g) Korevaar, P. A.; George, S. J.; Markvoort, A. J.; Smulders, M. M. J.; Hilbers, P. A. J.; Schenning, A. P. H. J.; De Greef, T. F. A.; Meijer, E. W. *Nature* **2012**, *481*, 492. (h) Lohr, A.; Lysetska, M.; Würthner, F. *Angew. Chem., Int. Ed.* **2005**, *44*, 5071.

(6) (a) de Groot, S. R.; Mazur, P. *Non-Equilibrium Thermodynamics*; Dover Publications: New York, 1984. (b) Demirel, Y. *Non-Equilibrium Thermodynamics, Transport and Rate Processes in Physical, Chemical and Biological Systems*, 2nd ed.; Elsevier B. V.: Amsterdam, 2007.

(7) Shigeno, M.; Sato, M.; Kushida, Y.; Yamaguchi, M. *Asian J. Org. Chem.* accepted, doi: 10.1002/ajoc.201402065.

(8) (a) Amemiya, R.; Saito, N.; Yamaguchi, M. *J. Org. Chem.* **2008**, *73*, 7137. (b) Saito, N.; Shigeno, M.; Yamaguchi, M. *Chem.—Eur. J.* **2012**, *18*, 8994. (c) Ichinose, W.; Ito, J.; Yamaguchi, M. *Angew. Chem., Int. Ed.* **2013**, *52*, 5290. (d) Amemiya, R.; Mizutani, M.; Yamaguchi, M. *Angew. Chem., Int. Ed.* **2010**, *49*, 1995. (e) Yamamoto, K.; Oyamada, N.; Mizutani, M.; An, Z.; Saito, N.; Yamaguchi, M.; Kasuya, M.; Kurihara, K. *Langmuir* **2012**, *28*, 11939.

(9) Yamaguchi, M.; Shigeno, M.; Saito, N.; Yamamoto, K. *Chem. Rec.* **2013**, *13*, 6.

(10) Shigeno, M.; Kushida, Y.; Yamaguchi, M. *Chem.—Eur. J.* **2013**, *19*, 10226.

(11) Newman, M. S.; Wolf, R. M. *J. Am. Chem. Soc.* **1956**, *78*, 450.

(12) For recent examples of stimuli-responsive single helix inversion, see: (a) Nagata, Y.; Yamada, T.; Adachi, T.; Akai, Y.; Yamamoto, T.; Suginome, M. *J. Am. Chem. Soc.* **2013**, *135*, 10104. (b) Freire, F.; Seco, J. M.; Quinoa, E.; Riguera, R. *Angew. Chem., Int. Ed.* **2011**, *50*, 11692. (c) Fukushima, T.; Tsuchihara, K. *Macromol. Rapid Commun.* **2009**, *30*, 1334. (d) Meudtner, R. M.; Hecht, S. *Angew. Chem., Int. Ed.* **2008**, *47*, 4926. (e) Sanda, F.; Terada, K.; Masuda, T. *Macromolecules* **2005**, *38*, 8149. (f) Ohira, A.; Kunitake, M.; Fujiki, M.; Naito, M.; Saxena, A. *Chem. Mater.* **2004**, *16*, 3919. (g) Li, J.; Schuster, G. B.; Cheon, K. S.; Green, M. M.; Selinger, J. V. *J. Am. Chem. Soc.* **2000**, *122*, 2603. For, stimuli response double-helix inversion, see: (h) Hasegawa, T.; Furusho, Y.; Katagiri, H.; Yashima, E. *Angew. Chem., Int. Ed.* **2007**, *46*, 5885.

(13) Helix inversion without external stimuli is known. For examples, see: (a) Gregoliński, J.; Lisowski, J. *Angew. Chem., Int. Ed.* **2006**, *45*, 6122. (b) Gregoliński, J.; Lis, T.; Cyganik, M.; Lisowski, J. *Inorg. Chem.* **2008**, *47*, 11527. (c) Abe, H.; Ohishi, Y.; Inouye, M. *J. Org. Chem.* **2012**, *77*, 5209. See also refs 5b, 5g, and 5h.

(14) The equilibrium constants $K_{hetero-C}$ = [random coil]^2/ [heterodouble helix] between random coil **A** and heterodouble helix **C** were obtained for a mixture of (P)-**1**/(M)-**2** in fluorobenzene (total 5.0×10^{-4} M) (SI Table S1): $K_{hetero-C} = 3.7 \times 10^{-6}$ M (25 °C) and $K_{hetero-C} = 1.9 \times 10^{-4}$ M (40 °C). The equilibrium constants $K_{homo-(M)-2}$ = [random coil]^2/[homodouble helix] between random coil and homodouble helix were obtained for (M)-**2** in fluorobenzene (2.5 × 10^{-4} M) (SI Table S2): $K_{homo-(M)-2}$ = 1.0×10^{-4} M (25 °C) and $K_{homo-(M)-2}$ = 4.3×10^{-3} M (40 °C).[7] The results showed the stronger heterointeractions between (P)-**1** and (M)-**2** compared with the homointeractions of (P)-**1** or (M)-**2**.

(15) For an example of thermal hysteresis in the solid state, see: (a) Kiriya, D.; Chang, H.-C.; Kitagawa, S. *J. Am. Chem. Soc.* **2008**, *130*, 5515. For an example of thermal hysteresis in neat liquid, see: (b) Terao, K.; Kikuchi, N.; Sato, T.; Teramoto, A.; Fujiki, M.; Dobashi,

T. *Langmuir* **2006**, *22*, 7975. For an example of thermal hysteresis of bulk polymers, see: (c) Liu, X.; Luo, S.; Ye, J.; Wu, C. *Macromolecules* **2012**, *45*, 4830. For an example of thermal hysteresis of aggregates, see: (d) Arai, F.; Ichikawa, A.; Fukuda, T.; Katsuragi, T. *Analyst* **2003**, *128*, 547. See also references cited in reference 10.

(16) Ross, J.; Villaverde, A. F. *Entropy* **2010**, *12*, 2199.

7980

dx.doi.org/10.1021/ja502009f | *J. Am. Chem. Soc.* 2014, 136, 7972−7980